A Novel Electrochromic Polyacetylene Derivative with Good Fluorescence Properties Electrodeposited by Direct Anodic Oxidation of 1,2-Methylenedioxybenzene

Jingkun Xu,*,†,‡ Houting Liu,†,‡ Shouzhi Pu,*,†,‡ Fuyou Li,§ and Mingbiao Luo‡

Jiangxi Key Laboratory of Organic Chemistry, Jiangxi Science and Technology Normal University, Nanchang 330013, China; College of Biology, Chemistry and Material Science, East China Institute of Technology, 56 Xuefu Road, Fuzhou 344000, China; and Department of Chemistry and Lab of Advanced Materials, Fudan University, Shanghai 200433, China

Received April 3, 2006; Revised Manuscript Received June 11, 2006

ABSTRACT: Direct anodic oxidation of 1,2-methylenedioxybenzene (MDOB), one of the analogues of 3,4-alkylenedioxythiophene and 3,4-alkylenedioxypyrrole, led to the formation of a novel polyacetylene derivative poly(1,2-methylenedioxybenzene) (PMDOB) on a platinum sheet in acetonitrile with good fluorescence properties of emissions at 390 and 410 nm, together with the electrochromic property from sap green (doped) to baby blue (dedoped). IR, ^{1}H NMR, ^{13}C NMR and quantum chemistry calculations confirmed the polymerization occurred at the C_4 and C_5 position on the benzene ring of the monomer, making the main backbone of PMDOB similar to polyacetylene. SEM results indicated the formation of aligned PMDOB nanorod on the electrode surface. The pressed PMDOB pellet has a conductivity of 0.8 S cm^{-1}. To the best of our knowledge, this is the first report on the electrochemical polymerization of MDOB and characterization of its polymer.

1. Introduction

The pursuit of high-quality polymer films is still one of the main goals in the research and development of inherently conducting polymers (CPs). Among the CPs studied during the past quarter century, poly(3,4-ethylenedioxythiophene) (PEDOT, Scheme 1), which has high conductivity, good processing ability, good mechanical property, and nice environmental stability, has become one of the most successful CPs from both a fundamental and practical perspective since its discovery in 1988.[1,2] The 3,4-alkylenedioxy group substitution at the β-position on the thiophene ring decreased the coupling defect through $\alpha-\beta$ positions, yielding regiosymmetric high-quality polymers. This facilitates the applications of PEDOT in various areas, such as antistatic coating, supercapacitors, electrode materials in organic light-emitting diodes, and solar cells.[3] The main drawback which limited the application of PEDOT was that the cost of their synthesis and further modification is too expensive. Considering the significant positive effect on the property enhancement of corresponding conducting polymers, the derivatives of 3,4-alkylenedioxy-substituted pyrroles (Scheme 1) had also been investigated.[4] However, the main drawback of these derivatives of polypyrrole was the relatively low oxidation potential of alkylenedioxy-substituted pyrrole monomers, which made them polymerize automatically in the air. This limited their further exploration. From the alkylenedioxy derivatives of polythiophene and polypyrrole, one question should be asked: how about the properties of other alkylenedioxy-substituted conducting polymers?

Besides polythiophenes and polypyrrole, poly(*p*-phenylene) (PPP) is also a very hot topic in CPs. Electrooxidative polymerization of heterocycles with concurrent polymer film deposition has been proved to be an especially useful method for the preparation of high-quality conducting polymer film.[5] Electrodeposited PPP has a high degree of orientation with almost fully coplanar rings. PPP generally was very purely para-polymerized.[6] However, the polymerization of alkylenedioxy-substituted benzene derivatives (Scheme 1) and characterization of its polymer had not been studied yet.

Scheme 1. Electrochemical Polymerization of Alkylenedioxythiophene, Alkylenedioxypyrrole, and Alkylenedioxybenzene

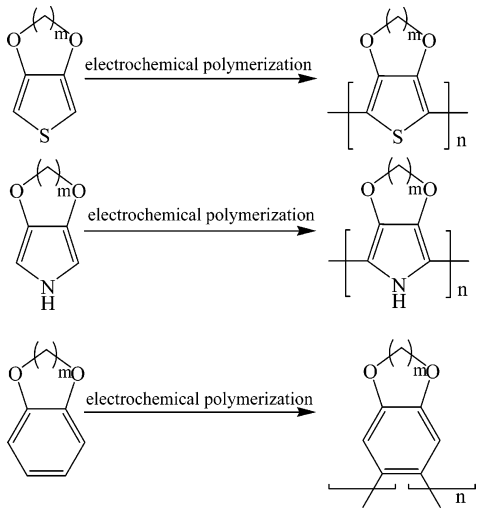

In this paper, the alkylenedioxy-substituted benzene was electrochemically polymerized for the first time. The main advantage for these monomers is their cheap commercial price. To our surprise, the structure of poly(alkylenedioxybenzene) was not similar to either poly(alkylenedioxythiophene) or PPP (Scheme 1). The main backbone of poly(1,2-methylenedioxybenzene) (PMDOB) was similar to polyacetylene, one of the simplest CPs. Furthermore, PMDOB film with good electrochromic properties, which transform from opaque sap green

† Jiangxi Science and Technology Normal University.
‡ East China Institute of Technology.
§ Fudan University.
* Corresponding authors. E-mail: xujingkun@tsinghua.org.cn, xujingkun@mail.ipc.ac.cn, or pushouzhi@singhua.org.cn.

10.1021/ma060742y CCC: $33.50
Published on Web 07/29/2006

(doped) to transparent baby blue (dedoped) together with good fluorescence properties, was easily prepared by direct anodic oxidation of 1,2-methlenedioxybenzene (MDOB) in acetonitrile (ACN) containing 0.1 mol L^{-1} Bu_4NBF_4. On the other hand, the polymerization of 1,2-ethylenedioxybenzene (EDOB) in the same electrolyte was not very successful on the electrode. The oligomer of poly(1,2-ethylenedioxybenzene) (PEDOB) attached to the electrode dissolved quickly during polymerization. Therefore, the polymerization mechanism, structural characterization, and the electrochemical behavior of PMDOB itself were determined in detail.

2. Experiment

2.1. Reagents and Treatment. MDOB, EDOB (Acros Organics), and commercial high-performance liquid chromatography grade acetonitrile (ACN, Beijing East Longshun Chemical Plant) were used directly without further purification. Bu_4NBF_4 (Acros Organics, 95%) was dried in a vacuum at 60 °C for 24 h before use. Dimethyl sulfoxide (DMSO) was a product of Beijing East Longshun Chemical Plant and was used directly.

2.2. Apparatus. The conductivity of as-formed PMDOB film was measured by the conventional four-probe technique with pressed pellets of the samples. UV−vis spectra were taken by using a Perkin-Elmer Lamda 900 UV−vis−NIR spectrophotometer. The infrared (IR) spectra were recorded by using KBr pellets of the polymers on the Bruker Vertex 70 FT-IR spectrometer. The fluorescence spectra were determined with an F-4500 fluorescence spectrophotometer (Hitachi). The ^1H NMR and ^{13}C NMR spectra were recorded on a Bruker AV 400 NMR spectrometer, and d_6-DMSO was used as the solvent. The thermogravimetric (TG) and differential thermogravimetric (DTG) analyses were performed with a thermal analyzer of Netzsch TG209. Scanning electron microscopy (SEM) measurements were taken by using a JEOL JSM-6360 LA analytical scanning electron microscope. The fluorescence quantum yields (ϕ) of PMDOB in solution was measured using anthrancene in ACN (standard, $\phi_{ref} = 0.27$)[7] as a reference and were calculated according to the well-known method given as

$$\phi_{overall} = \frac{n^2 A_{ref} I}{n_{ref}{}^2 A I_{ref}} \phi_{ref} \quad (1)$$

Here, n, A, and I denote the refractive index of solvent, the absorbance at the excitation wavelength, and the intensity of the emission spectrum, respectively. The subscript "ref" denotes the reference, and no subscript denotes the sample. Absorbances of the samples and the standard should be similar.[8]

The highest occupied molecular orbital (HOMO) energy level of the polymer was converted from the onset oxidation potential, with the assumption that the energy level of ferrocene/ferrocenium (Fc) is 4.8 eV below vacuum.[9]

2.3. Electrosyntheses of Polymer Films. Electrochemical syntheses and examinations were performed in a one-compartment cell with the use of model 263 potentiostat−galvanostat (EG&G Princeton Applied Research) under computer control. The working and counter electrodes were platinum wires with a diameter of 0.5 mm placed 0.5 cm apart. They were polished and cleaned by water and acetone successively before each examination. A typical electrolyte was ACN containing 0.1 mol L^{-1} Bu_4NBF_4, and the concentration of MDOB was 0.2 mol L^{-1}. All solutions were deaerated by a dry nitrogen stream and maintained under a slight overpressure during the experiments. The reference electrode was a platinum wire immersed directly into the electrolyte. It was calibrated using the ferrocene (Fc/Fc^+) redox couple which has a formal potential $E_{1/2} = +0.35$ V vs platinum wire in this medium.

3. Results and Discussion

3.1. Electrochemical Syntheses of PMDOB Films. Cyclic voltammetry (CV) is a very useful method which qualitatively reveals the reversibility of electron transfer during the electropolymerization and also examines the electroactivity of the polymer film because the oxidation and reduction can be monitored in the form of a current−potential diagram, i.e., CV diagram.[10] Figure 1 showed the CVs of 0.2 mol L^{-1} EDOB (A) and MDOB (B) in ACN containing 0.1 mol L^{-1} Bu_4NBF_4. As shown in Figure 1A, no apparent redox peak was found within five cycles, and PEDOB film deposited on the electrode solved quickly. During the polymerization, the color of the electrolyte became straw yellow quickly as CV scans proceeded. This implied the difficulty for the electrodeposition of PEDOB on the electrode.

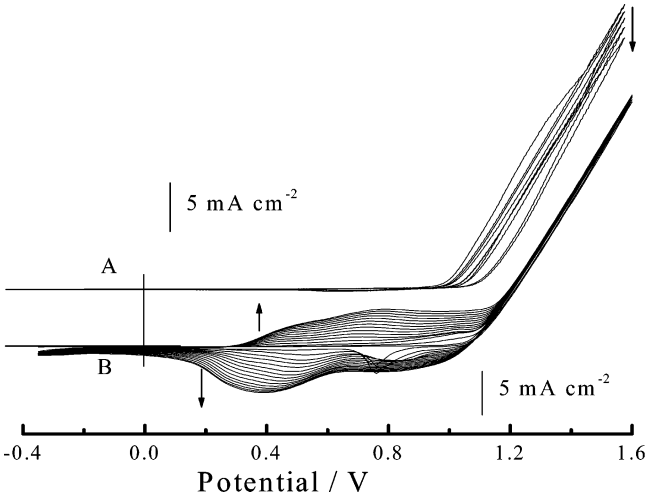

Figure 1. CVs of 0.2 mol L^{-1} EDOB (A) and 0.2 mol L^{-1} MDOB (B) in ACN contain 0.1 mol L^{-1} Bu_4NBF_4. Scanning rates: 150 mV s^{-1}.

On the other hand, there was an obvious reduction peak near 0.7 V in the first cycle for the CVs of MDOB (Figure 1B). In the second cycle, a slight break point started at 0.9 V, and an inconspicuous peak near 1.0 V in oxidized cycle formed. Two reductive peaks were found near 0.8 and 0.40 V, respectively. This pair of peaks was assigned to the transformation from quinoid structure to aromatic state. As the potential scanning continued, a polymer film was formed on the Pt electrode surface. PMDOB can be reduced and oxidized between 0.38 and 0.75 V. The increases of the redox wave currents implied that the amount of the polymer on the electrode increased. The potential shift of the wave current maximum provides information about the increase in the electrical resistance in the polymer film and the overpotential needed to overcome the resistance. All these phenomena indicated that high-quality PMDOB film was formed on the electrode. Because of the difficulty for the electrodeposition of PEDOB, the following studies were mainly focused on PMDOB.

3.2. Electrochemistry of PMDOB Films. The electrochemical behavior of as-formed PMDOB films was determined in monomer-free ACN containing 0.1 mol L^{-1} Bu_4NBF_4 (Figure 2). The steady-state cyclic voltammograms represented two couple of redox peaks in slow scanning rate (25 mV s^{-1}). The redox peaks were centered at 0.52 and 0.71 V, which can be mainly ascribed to the switch from para-quinoid to doped aromatic state. Following the increases of scanning rate, this switch became unobvious. This was mainly due to the scanning rate was faster than transformation from para-quinoid state to doped aromatic state. The peak current densities were proportional to the scan rates (inset of Figure 2), indicating good redox activity of the polymer.[11] Furthermore, these films could be cycled repeatedly between the conducting (oxidized) and

CDV

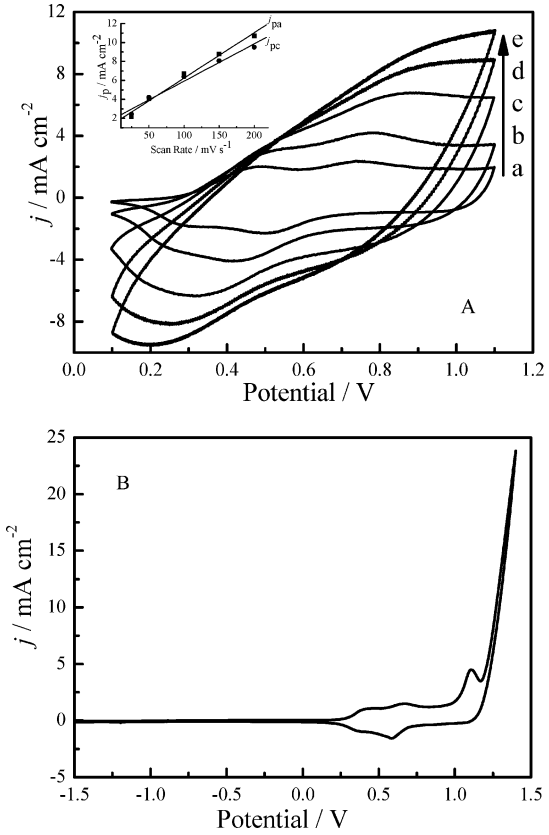

Figure 2. (A) Cyclic voltammograms of PMDOB films in ACN containing 0.1 mol L^{-1} Bu_4NBF_4 in the potential range of 0.1−1.1 V at potential scan rates of 25 (a), 50 (b), 100 (c), 150 (d), and 200 mV s^{-1} (e). (B) Cyclic voltammograms of PMDOB films in ACN containing 0.1 mol L^{-1} Bu_4NBF_4 in the potential range of −1.5 to 1.4 V at potential scan rate of 50 mV s^{-1}. The films were synthesized electrochemically in ACN containing 0.1 mol L^{-1} Bu_4NBF_4 at a constant applied potential of 1.4 V.

insulating (neutral) states without significant decomposition of the materials, indicating the high structural stability of the polymer. The oxidation potential onset of PMDOB was observed at +0.83 V (Figure 2B). Since the energy level of ferrocene/ferrocenium (Fc) is determined by photoelectron spectroscopy in the solid state as −4.8 eV, this method can only be considered to be a rough approximation.[9] The HOMO energy of PMDOB was estimated to be −5.63 eV. There was no reduction potential because of the unstable of PMDOB during negative potential scanning. Therefore, the LUMO of PMDOB cannot be estimated directly by the electrochemical method.

3.3. Structural Characterizations. PMDOB can be thoroughly dissolved in a strong polar solvent such as DMSO. However, it cannot be dissolved in a common organic solvent such as tetrahydrofuran, CH_2Cl_2, chloroform, DMF, etc. For characterization of the structure and properties of as-formed polymers, UV−vis, fluorescence, IR, and ^1H NMR and ^{13}C NMR spectra of the polymer were determined.

The doped and dedoped PMDOB dissolved in DMSO was orange. Figure 3 showed the UV−vis spectra of monomer (A), doped (B) and dedoped (C) PMDOB in DMSO. Similar to the absorption of monomer, the polymer also showed strong absorption at 282 nm, as shown in Figure 3. At the same time another wide absorption of PMDOB can also be found from 302 to 360 nm. Generally, higher wavelength means higher conjugation length. Therefore, the result of the red shift of UV−vis spectra of PMDOB means higher conjugation backbone in comparison with the monomer.[12] In comparison with dedoped

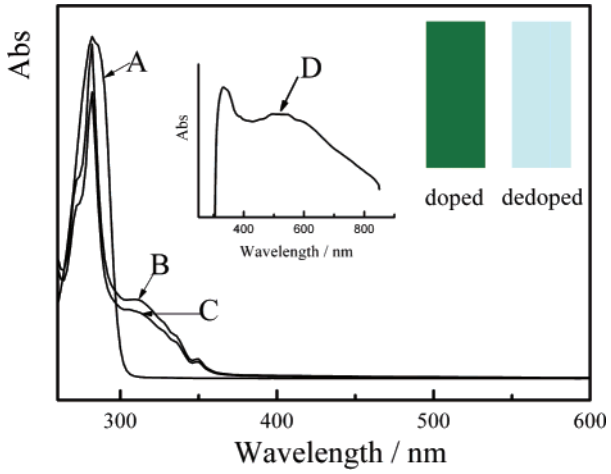

Figure 3. UV−vis spectra of MDOB (A), doped PMDOB (B), and dedoped PMDOB (C) prepared from ACN containing 0.1 mol L^{-1} Bu_4NBF_4 and 0.2 mol L^{-1} MDOB. Solvent: DMSO. Inset: UV−vis spectrum of doped PMDOB film on ITO electrode (D).

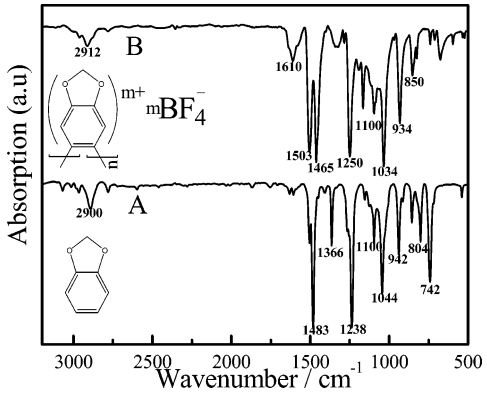

Figure 4. FTIR spectra of the MDOB (A) and doped PMDOB (B) obtained potentiostatically at 1.4 V from ACN containing 0.1 mol L^{-1} Bu_4NBF_4 and 0.2 mol L^{-1} MDOB.

PMDOB in solution (Figure 3C), the spectrum of doped PMDOB was quite similar (Figure 3B). This is mainly caused by the automatic dedoping process of PMDOB in DMSO solution. However, the doped PMDOB film showed another strong absorption on the ITO electrode, from 430 to 850 nm with a peak centered at ca. 530 nm (Figure 3D). This wide peak can be assigned to the absorption of conductive species on the main backbone of PMDOB in the doped state.

On the other hand, PMDOB also showed good electrochromic properties between the doped and dedoped state, from sap green to baby blue, respectively (Figure 3 inset). However, the electrochromic stability of PMDOB on the electrode in ACN was not very good, maybe because of the short conjugation length of PMDOB in comparison with those popular conducting polymer together with the moving in/out of counterions during the doping and dedoping processes. The band gap of PMDOB obtained from optical absorption edge was 3.26 eV.[8] Therefore, the LUMO energy level can be estimated by band gap and HOMO as −2.37 eV (band gap = LUMO−HOMO). It should be mentioned that obtaining absolute HOMO and LUMO levels from electrochemical data in combination with the energy gap is still under debate.[9]

Figure 4 showed the infrared spectra of MDOB (A) and PMDOB (B) in the doped state. From this figure, obvious changes were found between the monomer and polymer. Typical peaks centered at 2900, 1483 cm^{-1} in monomer (Figure 4A) and 2912, 1465 cm^{-1} in polymer (Figure 4B) assigned to the

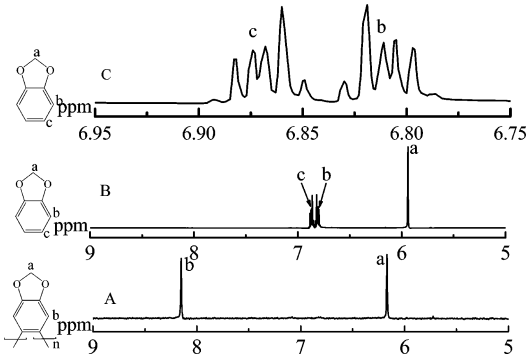

Figure 5. ^{1}H NMR spectra of PMDOB (A) and MDOB (B). Solvent: d_6-DMSO.

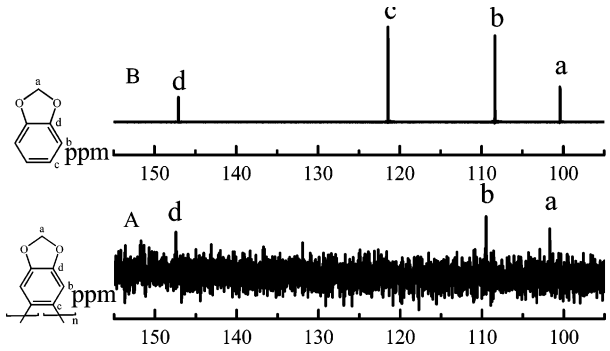

Figure 6. ^{13}C NMR spectra of PMDOB (A) and MDOB (B). Solvent: d_6-DMSO.

stretching of $-CH_2-$ and vibration of C−C in aromatic ring. The C−O−C asymmetry stretching of MDOB and PMDOB appeared at 942 and 934 cm^{-1}, respectively. All the above illustrates that the aromatic ring and the C−O−C band were not destroyed during electrochemical polymerization. The peaks of MDOB, centered at 742 cm^{-1} and multiplet from 2000 to 1600 cm^{-1}, were assigned to the 1,2-disubstituted of aromatic ring (Figure 4A). However, these peaks changed significantly in the spectrum of the polymer (Figure 4B). The double peaks were centered at 1600, 1503 cm^{-1} and a single peak was centered at 850 cm^{-1}, indicating a 1,2,4,5-substituted benzene ring. These results imply that polymerization of MDOB may occur at the C_4 and C_5 position.

To further explicit the structure of PMDOB, the ^{1}H NMR (Figure 5A) and ^{13}C NMR (Figure 6A) spectra of PMDOB in d_6-DMSO were recorded by a Bruker AV 400 NMR spectrometer. For comparison, the ^{1}H and ^{13}C NMR spectra of the monomer were also included (Figure 5B,C and Figure 6B). Three proton groups can be found in the ^{1}H NMR spectrum of MDOB: 5.9, 6.79−6.83, and 6.85−6.88, which can be assigned to the protons at the methylene (Figure 5B), b, and c positions (Figure 5C), respectively. Because of the spin−spin splitting between protons at b and c positions, they both showed multiple peaks (Figure 5C). In the spectrum of PMDOB, there was only one singlet at 8.15 ppm. There may be three polymerization mechanisms for the electrochemical polymerization of MDOB, through b−b, b−c, and c−c positions. If the polymerization happened through b−b or b−c, the proton lines would be a triplet. Therefore, this singlet proton line at 8.15 ppm can be assigned to the protons at the b position. This implies that the polymerization site was the c position (C_4 and C_5), and the main backbone of PMDOB was similar to polyacetylene (Scheme 1). In addition, the chemical shift at 8.15 and 6.17 ppm moving to lower field indicated higher conjugation length in comparison with those of the monomer.[13] Four group peaks can be found

Table 1. Main Atomic Electron Density Populations for MDOB

atom	electric charge	atom	electric charge
C_1	0.252394	C_2	0.252372
C_3	−0.106342	C_4	−0.141507
C_5	−0.141497	C_6	−0.106349
C_7	0.195729		

Table 2. Main Composition and Proportion of the Frontier Orbitals in MDOB (%)

atom	HOMO−1	HOMO	LUMO	LUMO+1
C_1	0.040482	0.138078	0.097019	0.200874
C_2	0.040491	0.138083	0.097023	0.200863
C_3	0.297939	0.015842	0.311251	0.001481
C_4	0.074003	0.118812	0.070741	0.266536
C_5	0.074018	0.118794	0.070734	0.266543
C_6	0.297931	0.015852	0.311251	0.001482
C_7	0.000002	0.012764	0.000191	0.000019

Scheme 2. Structural Formula of Calculated MDOB

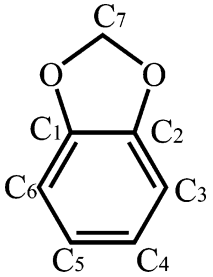

in ^{13}C NMR of MDOB (Figure 6B): 100, 108, 121, and 147 ppm, which can be assigned in a, b, c, and d in Figure 6B, respectively. Although the peak intensity became weak after polymerization, three group peaks at 101, 109, and 147 ppm can also be found in Figure 6A. The peak of MDOB in 121 ppm disappeared in ^{13}C NMR of PMDOB (Figure 6A), which was mainly due to the strength of C_c becoming weak following its transition from a tertiary carbon to quaternary carbon during the polymerization, in well agreement with the results of ^{1}H NMR.

To get deep insight into PMDOB structures and the polymerization mechanism, the atomic electron density population and reactivity of MDOB monomer (Scheme 2) were also calculated at the B3LYP/6-31G (d,p) level using Hyperchem software. The results of main atomic electron density populations showed negative electric charges on C(3), C(4), C(5), and C(6) (Table 1), which implied that these atoms will donate electrons when MDOB monomer during electrochemical polymerization through radical cation intermediates. According to the molecular orbital theory, the reaction between the active molecules mainly happens on the frontier molecular orbital and near orbital. For

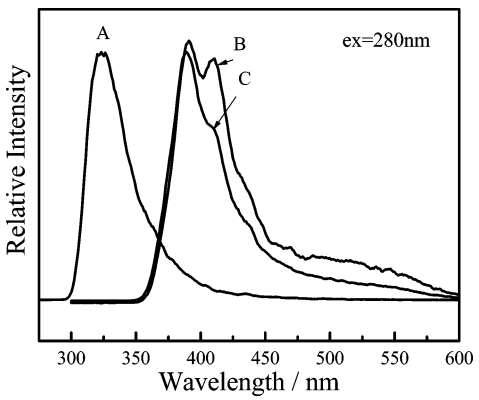

Figure 7. Emission spectra of MDOB (A), doped PMDOB (B), and dedoped PMDOB (C) in DMSO.

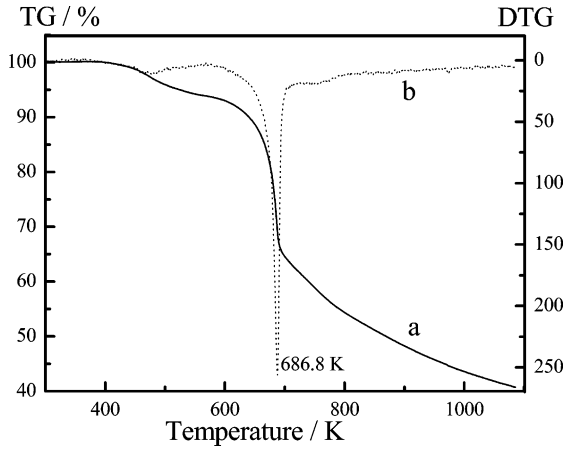

Figure 8. TGA curves of dedoped PMDOB films obtained potentiostatically at 1.4 V from ACN containing 0.1 mol L^{-1} Bu_4NBF_4 and 0.2 mol L^{-1} MDOB after dedoping at −0.2 V until current was close to zero.

MDOB, the proportions of atoms C(1), C(2), C(4) and C(5) in HOMO were higher than other atoms as listed in Table 2. At the same time, C(3), C(4), C(5), and C(6) also had rich negative charges (Table 1). These theoretical results implied that the polymerization between the monomer would happen preferentially on C(4) and C(5), in well accordance with the results of IR, ^1H NMR and ^{13}C NMR. All these results indicated PMDOB is one of the derivatives of polyacetylene, not PPP.

The photoluminescence properties of PMDOB were also measured. As shown in Figure 7, an obvious emission peak at 390 and 410 nm was found in the fluorescence spectra of doped (Figure 7B) and dedoped (Figure 7C) PMDOB, respectively. For the monomer, it was located at 320 nm (Figure 7A). The red shift of the emission peak further proved the formation of conjugated backbone of PMDOB, in well agreement with the UV−vis spectral results (Figure 4). The difference between doped and dedoped PMDOB may be the effect of counterion. These results imply that PMDOB may be a good candidate in blue-light-emitting material, since it is very difficult to achieve blue-light-emitting materials.[14] The fluorescence quantum yield of as-formed PMDOB in DMSO was measured to be 0.13 according to eq 1.

3.4. Thermal Analysis. The thermal analysis was performed under a nitrogen stream from 293 to 1128 K with a heating rate of 10 K/min (Figure 8). The structure of PMDOB main backbone was kept up to 691 K. There was three-step loss of weight (Figure 8A). The first one is from 413 to 559 K, up to 5.97%, which can be ascribed to water evaporation or other moisture trapped in the polymer. The second one occurred from 559 to 691 K, up to 28.44%, which was attributed the degradation of the skeletal PMDOB backbone chain structure.

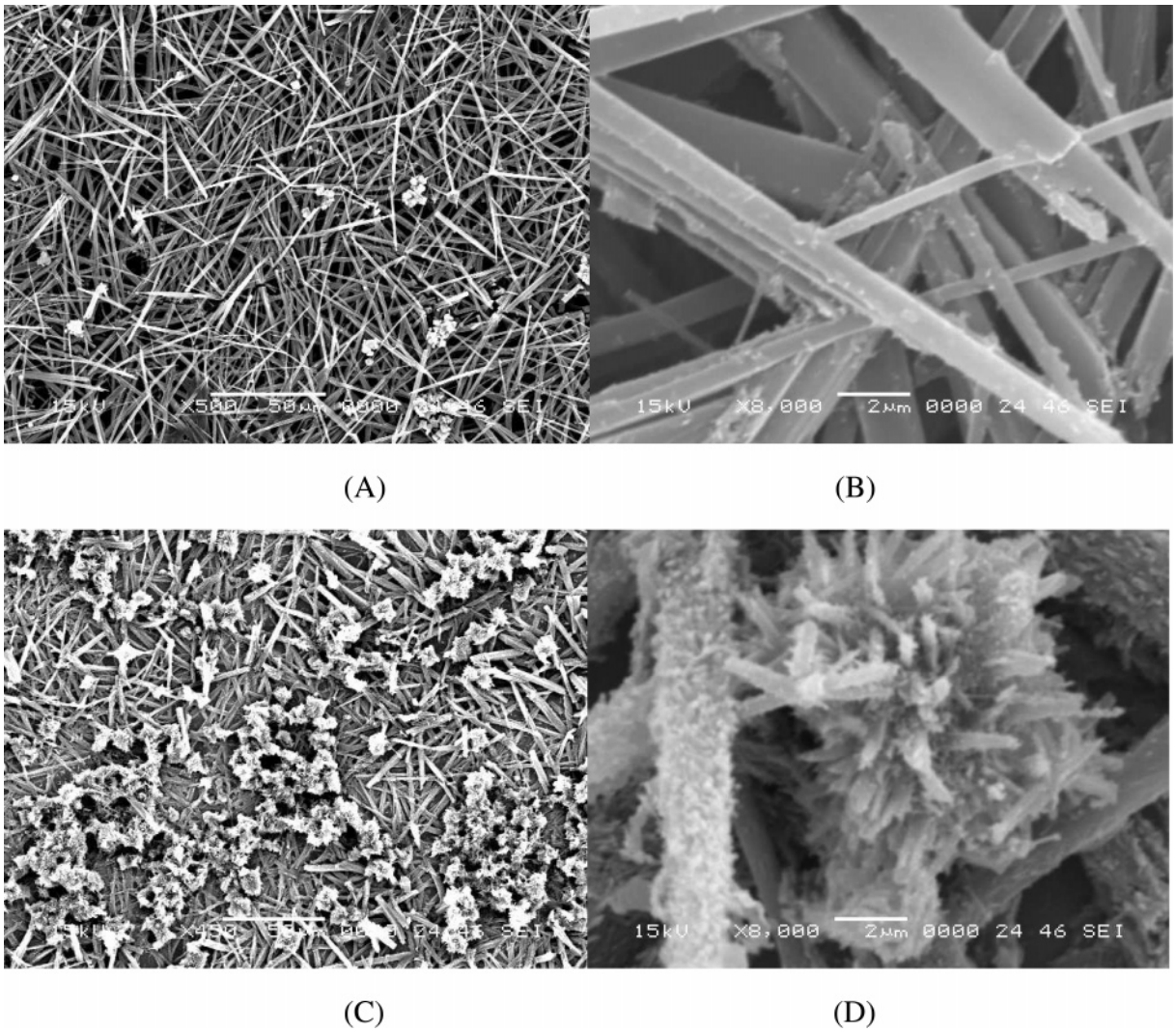

Figure 9. SEM micrographs of PMDOB film deposited on the ITO glass electrode surface from ACN containing 0.1 mol L^{-1} Bu_4NBF_4 at applied potential of 1.4 V. (A) and (B): doped; (C) and (D): dedoped.

The last one was about 66.19% from 693 to 1085 K, possibly owing to the overflow of some oligomers that decomposed from the PMDOB. From the DTG curves (Figure 8B), the fastest weight change rate of PMDOB films occurred at 686.8 K. All these results indicated that PMDOB had good thermal stability.

3.5. Morphology and Conductivity. The typical SEM images of PMDOB films are shown in Figure 9. The doped PMDOB film was an aligned nanorod with a diameter of 100−2000 nm (Figure 9A,B). Partly coralloid cluster embellished on the surface during electrodeposition. The surface of coralloid cluster was a distribution of hole with a diameter about 100 nm. After dedoping at a constant applied potential of −0.2 V, the surface of PMDOB film became uneven (Figure 9C,D). This was due to the migration of counteranion out of the polymer surface, which broke the smooth surface of these nanorods. The coralloid cluster was much enriched than doped PMDOB, and the hole appeared as belemnoid. The main reason for the production of PMDOB nanorods may be ascribed to the self-assembly of MDOB monomer on Pt electrode in ACN. Generally, the production of nanomaterials through electrochemical method needs templates such as Al_2O_3 or polycarbonate or using a template-free method.[15] During the polymerization of MDOB in ACN + 0.1 mol L^{-1} Bu_4NBF_4, no template and no surfactants were used. Therefore, the formation of PMDOB nanorod should be a template-free approach. The usage of ITO electrode acted as nucleation center and self-assembly occurred around these centers, and PMDOB nanorod was formed on the electrode surface. This is a facile method for the production of PMDOB nanomaterials.

The conductivity of pressed PMDOB pellets from ACN was measured to be 0.8 S cm^{-1}, making PMDOB good semiconducting materials.

4. Conclusion

In summary, a novel conducting polymer PMDOB with electric conductivity of 0.8 S cm^{-1} through pressed pellets of the samples, whose main backbone was similar to polyacetylene, with good fluorescence property were easily electrochemically deposited by direct anodic oxidation of MDOB in ACN containing 0.1 mol L^{-1} Bu_4NBF_4. UV−vis, FT-IR, ^1H NMR, ^{13}C NMR, and quantum chemistry calculations determined the structure of PMDOB as a polyacetylene derivative. Furthermore, PMDOB owns good thermal stability. As-formed PMDOB on ITO electrode was nanorod. To the best of our knowledge, this is the first report on the electrochemical polymerization of MDOB and characterization of its polymer.

Acknowledgment. Nanchang University testing fund (2005013), Funds of Jiangxi Provincial Department of Education ([2006]243), and NSFC (20564001) are acknowledged for their financial support.

References and Notes

(1) (a) Jonas, F.; Schrader, L. *Synth. Met.* **1991**, *831*, 41−43. (b) Heywang, G.; Jonas, F. *Adv. Mater.* **1992**, *4*, 116−118. (c) Winter, L.; Reece, C.; Hormes, J.; Heywang, G.; Jonas, F. *Chem. Phys.* **1995**, *194*, 207−213. (d) Hietrich, M.; Heinze, J.; Heywang, G.; Jonas, F. *J. Electroanal. Chem.* **1994**, *369*, 87−92.

(2) (a) Cutler, C. A.; Bouguettaya, M.; Kang, T. S.; Reynolds, J. R. *Macromolecules* **2005**, *38*, 3068−3074. (b) Welsh, D. M.; Kloeppner, L. J.; Madrigal, L.; Pinto, M. R.; et al. *Macromolecules* **2002**, *35*, 6517−6525. (c) Sotzing, G. A.; Thomas, C. A.; Reynolds, J. R. *Macromolecules* **1998**, *31*, 3750−3752 (d) Wang, F.; Wilson, M. S.; R.; Rauh, D. *Macromolecules* **2000**, *33*, 2083−2091.

(3) (a) Groenendaal, L.; Jonas, F.; Freitag, D.; Pielartzik, H.; Reynolds, J. R. *Adv. Mater.* **2000**, *12*, 481−494. (b) Groenendaal, L.; Zotti, G.; Auber, P. H.; Waybright, S. M.; Reynold, J. R. *Adv. Mater.* **2003**, *15*, 855−879. (c) Xu, J. K.; Pu, S. Z.; Shen, L.; Xiao, Q. *Chem. Res.* **2005**, *16* , 94−98.

(4) (a) Gaupp, C. L.; Zong, K.; Schotland, P.; Thompson, B. C.; Thomas, C. A.; Reynolds, J. R. *Macromolecules* **2000**, *33*, 1132−1133. (b) Schottland, P.; Zong, K.; Gaupp, C. L.; Thompson, B. C.; Thomas, C. A.; Reynolds, J. R. *Macromolecules* **2000**, *33*, 7051−7061. (c) Zong, K.; Reynolds, J. R. *J. Org. Chem.* **2001**, *66*, 6873−6882.

(5) Novak, P.; Muller, K.; Santhanam, S. V.; Haas, O. *Chem. Rev.* **1997**, *97*, 207−28.

(6) (a) Berresheim, A. J.; Muller, M.; Mullen, K. *Chem. Rev.* **1999**, *99*, 1747−1785. (b) Sim, I. S.; Kim, J. W.; Choi, H. J.; Kim, C. A.; Jhon, M. S. *Chem. Mater.* **2001**, *13*, 1243−1247. (c) Baskar, C.; Lai, Y.-H.; Valiyaveettil, S. *Macromolecules* **2001**, *34*, 6255−6260. (d) Manna, A.; Bandyopadhyay, K.; Vijayamohanan, K.; Rajamohanan, P. R.; Sainkar, S.; Kulkarni, B. D. *Langmuir* **1998**, *14*, 84−90. (e) Zhang, R.; Zheng, H.; Shen, J. *Macromolecules* **1996**, *29*, 7627−7628.

(7) Zimmermann, C.; Mohr, M.; Zipse, H.; Eichberger, R.; Schnabel, W. *J. Photochem. Photobiol. A: Chem.* **1999**, *125*, 47−56.

(8) Tasi, F. C.; Chang, C. C.; Liu, C. L.; Chen, W. C.; Jenekhe, S. A. *Macromolecules* **2005**, *38*, 1958−1966.

(9) (a) Pommerehne, J.; Vestweber, H.; Guss, W.; Mahrt, R. F.; Bassler, H.; Porsch, M.; Daub, J. *Adv. Mater.* **1995**, *7*, 551−554. (b) Zhang, X. W.; Liu, Y. Q.; Wu, X.; Wang, S.; Zhu, D. B. *Macromolecules* **2002**, *35*, 2529−2537. (c) Li, H. C.; Lambert, C.; Stabl, R. *Macromolecules* **2006**, *39*, 2049−2055.

(10) Li, X. G.; Huang, M. R.; Duan, W.; Yang, Y. L. *Chem. Rev.* **2002**, *102*, 2925−3030.

(11) (a) Skotheim, T. A. *Handbook of Conducting Polymer*; Marcel Dekker: New York, 1986. (b) Skotheim, T. A.; Elsembaumer, R. L.; Reynolds, J. R. *Handbook of Conducting Polymer*, 2nd ed.; Elsevier: New York, 1998.

(12) Sak-Bisnar, M.; Budimir, M.; Kovac, S.; Kukulj, D.; Duic, L. *J. Polym. Sci., Polym. Chem.* **1992**, *30*, 1609−1614.

(13) (a) Xu, J. K.; Nie, G. M.; Zhang, S. S.; Han, X. J.; Hou, J.; Pu, S. Z. *J. Polym. Sci., Polym. Chem.* **2005**, *43*, 1444−1453. (b) Xu, J. K.; Hou, J.; Zhou, W. Q.; et al. *Spectrochim. Acta, Part A* **2006**, *63*, 723−728. (c) Xu, J. K.; Zhou, W. Q.; Hou, J.; et al. *J. Polym. Sci., Polym. Chem.* **2005**, *43*, 3986−3997. (d) Xu, J. K.; Hou, J.; Zhang, S. S.; et al. *Eur. Polym. J.* **2006**, *42*, 1384−1395. (e) Xu, J. K.; Zhou, W. Q.; Hou, J.; et al. *Chin. J. Polym. Sci.* **2006**, *24*, 47−52. (f) Xu, J. K.; Hou, J.; Zhang, S. S.; et al. *J. Phys. Chem. B* **2006**, *110*, 2643−2648. (g) Xu, J. K.; Zhang, Y. J.; Hou, J.; et al. *Eur. Polym. J.* **2006**, *42*, 1154−1163. (h) Xu, J. K.; Hou, J.; Pu, S. Z.; et al. *J. Appl. Polym. Sci.* **2006**, *101*, 539−547. (i) Xu, J. K.; Zhou, W. Q.; Hou, J.; et al. *Mater. Lett.* **2005**, *59*, 2412−2417.

(14) (a) Scherf, U.; List, E. J. W. *Adv. Mater.* **2002**, *14*, 477−487. (b) Leclerc, M. *J. Polym. Sci., Part A: Polym. Chem.* **2001**, *39*, 2867−2873. (c) Neher, D. *Macromol. Rapid Commun.* **2001**, *22*, 1365−1385. (d) Morin, J. F.; Leclerc, M.; Ades, D.; Siove, A. *Macromol. Rapid Commun.* **2005**, *26*, 761−778.

(15) (a) Cho, S. I.; Kwon W. J.; Choi S. J.; et al. *Adv. Mater.* **2005**, *17*, 171−175. (b) Fu, M. X.; Zhu, Y. F.; Tan, R. Q.; Shi, G. Q. *Adv. Mater.* **2001**, *13*, 1874−1877. (c) Yang, Y. S.; Wan, M. X. *J. Mater. Chem.* **2002**, *12*, 897−901. (d) Yang, Y. S.; Wan, M. X. *J. Mater. Chem.* **2001**, *11*, 2022−2027. (e) Liu, J.; Wan, M. X. *J. Mater. Chem.* **2001**, *11*, 404−407.

MA060742Y